

# Numerical simulations of the acoustic noise radiated by radial fans

Hakan Dogan<sup>1</sup>, Martin Ochmann<sup>2</sup>, Chris Eisenmenger<sup>3</sup>, Stefan Frank<sup>4</sup>

<sup>1</sup> Beuth Hochschule für Technik, 13353 Berlin, E-Mail: [hdogan@beuth-hochschule.de](mailto:hdogan@beuth-hochschule.de)

<sup>2</sup> Beuth Hochschule für Technik, 13353 Berlin, E-Mail: [ochmann@beuth-hochschule.de](mailto:ochmann@beuth-hochschule.de)

<sup>3</sup> Hochschule für Technik und Wirtschaft, 12459 Berlin, E-Mail: [c.eisenmenger@htw-berlin.de](mailto:c.eisenmenger@htw-berlin.de)

<sup>4</sup> Hochschule für Technik und Wirtschaft, 12459 Berlin, E-Mail: [stefan.frank@htw-berlin.de](mailto:stefan.frank@htw-berlin.de)

## Introduction

The reduction of the acoustic noise caused by rotating radial fans is of importance in many engineering applications. In general, a broadband noise spectrum is observed with a major noise component at the blade passing frequency of the fan [1], and further contributions from the wall reflections and the vortex-induced waves. The unsteady and turbulent physics of the flow implies that the near field propagation should be solved by means of transient computational fluid dynamics methods, for the initial rotations of the fan [2, 3]. Such results regarding the pressure and the velocity variations in the fluid can be then used with the so called ‘acoustic analogy’ to estimate the acoustic noise in the far field.

In this work, the acoustic noise from a rotating fan used in a household dryer is investigated. For the present analysis, a laboratory scale fan with a rotor section with 8 backward curved blades is considered. The housing of the fan which encases the rotor is designed as a logarithmic spiral to provide a smooth air flow and to ensure a higher efficiency. Figure 1 shows the geometry, the backward curved blades, the housing and the outlet of the radial fan considered in the calculations displayed by using the COMSOL software [4].

The compressible flow within the fan is solved via a commercial software, e.g. ANSYS [5]. Using the results obtained from the computational fluid dynamics (CFD) simulations, the acoustic pressure distribution within the fan is then predicted with a computational acoustics code. The method used for the acoustic computation is the Boundary Element Method (BEM) (developed in Ref. [6]) which is employed over a virtual Kirchhoff surface near the blades (see the part denoted as ‘Imaginary Boundary’ in Fig. 1), the rigid walls (housing) and the outlet of the fan.

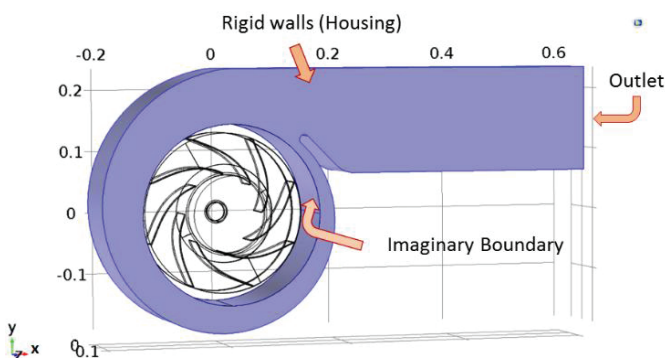


**Figure 1:** The geometry of the fan showing the rotor and the blades transparently, and the other surfaces. The Imaginary Boundary is a virtual interface which aids data exchange between the rotary part and the rest of the fan.

## Computational methods

As mentioned in the Introduction, a hybrid CFD/BEM approach is used in this work in order to compute the acoustic sound pressure level within a radial fan. Namely, first the CFD simulations are performed for some initial rotations of rotor section (e.g. 6 or 8 revolutions) using the ANSYS software. The time history of the pressure fluctuations on the rigid walls and at the outlet of the fan can be readily obtained from the ANSYS simulations. Furthermore, a virtual surface outside the rotor blades is also formed in the CFD simulations and the time domain variations of the pressure on that surface is monitored. Hence, these three surfaces (depicted as the blue region in Fig. 1) constitute the boundaries of the domain for the acoustic calculations. The pressure data on these surfaces are transformed into frequency domain using Fast Fourier Transform (FFT), and used in the BEM calculation to determine the acoustic pressure amplitude at any interior point inside the fan. Only the pressure fluctuations on the boundary (dipole sources) are considered and the volume fluctuations (quadrupole sources which are normally formulated through the Lighthill stress tensor) are neglected. In Ref. [7], it was shown that the effects of the quadrupoles for problems which involve small Mach numbers (as in this work as it will be clarified below) are negligible.

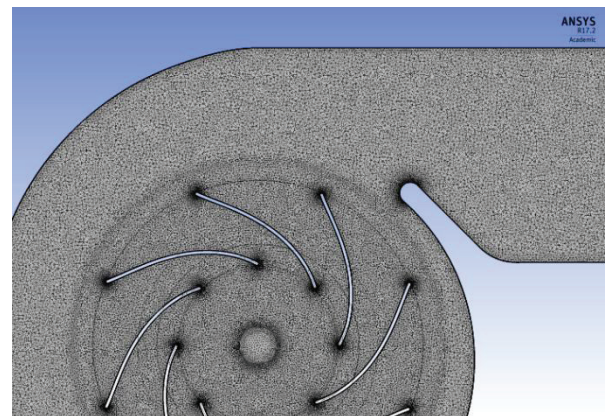


**Figure 2:** An example of the CFD mesh created in ANSYS with tetrahedral elements ( $x$ - $y$  cross-section, see Fig. 1).

## CFD computations

To obtain an accurate solution by means of computational fluid methods is a challenging task, especially for the fluid-structure interaction type problem considered here, which involves turbulent boundary layers at the rotating and the stationary surfaces. Hence, a few different methods have been tried so far in this work which include: Shear stress transport based Scale Adaptive Simulation (SST-SAS),

Detached Eddy Simulation (DES) and Stress-Blended Eddy Simulation (SBES).

The boundary condition at the inlet of the fan is prescribed as the volumetric flow rate  $\dot{V}=800 \text{ m}^3/\text{h}$ , which is in  $-z$  direction (see Fig. 1) through the front surface of the fan near the rotor. The rotational speed is set as  $n=3000$  rotations per minute (rpm). The relative pressure at the outlet of the fan is set to be 0 Pa so that the pressure difference between the inlet and the outlet yields the pressure rise ( $\Delta p$ ) of the fan.

The CFD mesh for the SST-SAS and the SBES consisted of approximately 28 to 29 million nodes with tetrahedral elements. The transition along the boundary layers has been resolved with 12-15 prism layers. A detailed view of the mesh in the  $x$ - $y$  cross-section can be seen in Fig. 2. The time step is chosen as equivalent to  $1^\circ$  or  $2^\circ$  rotation of the fan (depending on the turbulence model used), which corresponds to  $\Delta t=5.5 \times 10^{-5} \text{ s}$  and  $\Delta t=1.1 \times 10^{-4} \text{ s}$ , respectively.

For the prescribed operating conditions above, the torque  $M$  is computed approximately as 0.90 N m in the simulations. The static efficiency can be calculated using the static pressure rise and the torque of the fan via the equation:

$$\eta_{st} = \frac{\dot{V} \Delta p}{M 2\pi n}. \quad (1)$$

The results from the SST-SAS and the DES simulations have predicted the theoretical static efficiency given in Eq. (1) as 77.3% and 78.3%, respectively.

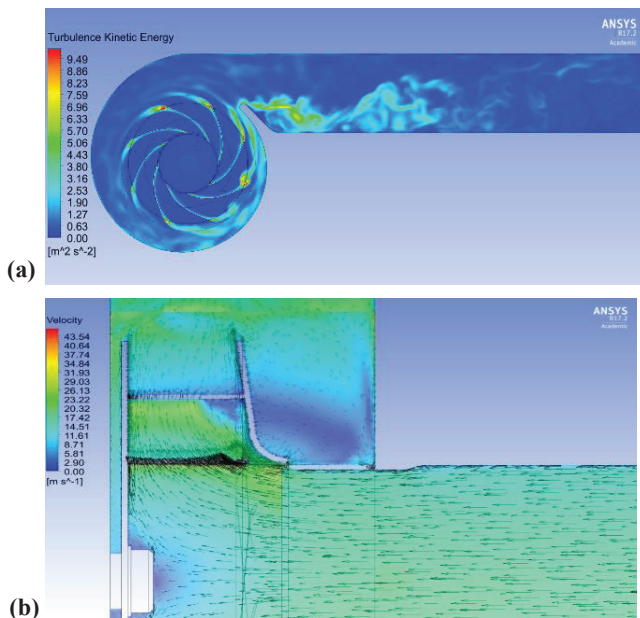


**Figure 3:** The results of the SST-SAS simulation. Turbulent kinetic energy in the  $x$ - $y$  cross-section of the fan is shown in (a) and the velocity vectors in a  $x$ - $z$  plane cut near the rotor are shown in (b).

Clearly, it is possible to monitor many variables during the CFD simulations such as the pressure, density, acoustical

Mach number, turbulent kinetic energy etc. In Fig. 3, some representative results are presented. For instance, Fig. 3a displays the turbulent kinetic energy distribution inside the fan plotted over the  $x$ - $y$  plane. It can be seen that the most turbulent regions are the tips of the blades and the wake region behind the volute tongue. Furthermore, the velocity vectors in the  $x$ - $z$  cross-section (from the top view) are shown in Fig. 3b. One can observe that the fluid is drastically accelerated near the blade tips. Although not included as a separate figure, the results have shown that the acoustical Mach number is less than 0.11 throughout the whole domain.

### Acoustic computations

The acoustic pressure distribution and the propagation modes within the fan can be found in the frequency domain by solving the Helmholtz equation:

$$\nabla^2 p + k^2 p = 0, \quad (2)$$

where  $p$  is the pressure and  $k=\omega/c$  is the wavenumber with  $\omega$  being the angular frequency and  $c$  denoting speed of sound in air. As mentioned above, the domain for the acoustic calculation is prescribed as the region between the Imaginary Boundary and the outlet of the fan, enclosed by the rigid wall along the duct. Therefore, the CFD results obtained on these boundaries for pressure are converted into frequency domain using the FFT, and Eq. (2) is then solved at each of the discrete frequencies. Before proceeding to such computation, an example test problem is given below in order to validate the acoustic solver.

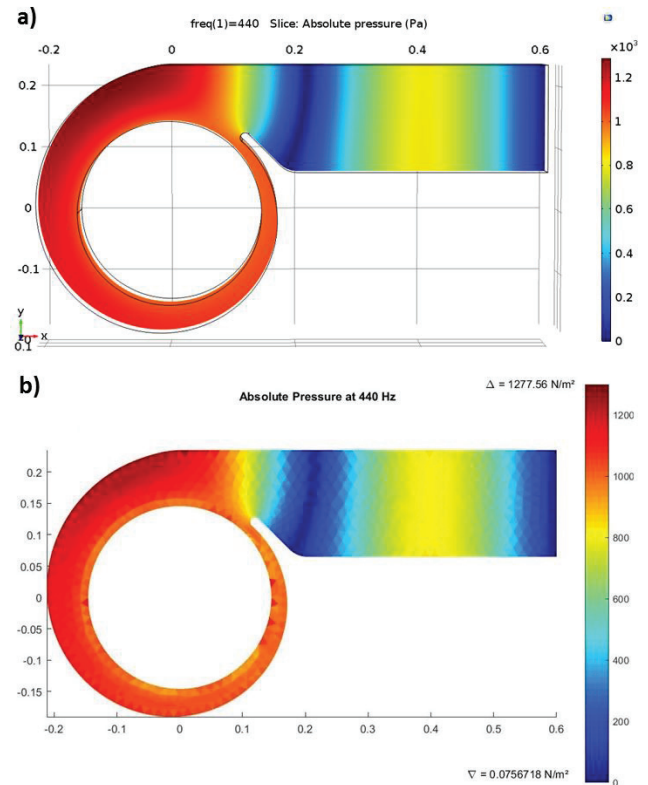


**Figure 4:** The results for the acoustic pressure distribution at 440 Hz for the test problem. (a) The solution with COMSOL, and (b) the solution with BEM.

**Test problem**

The numerical algorithm for solving Eq. (2) can be validated with a test problem which is created by choosing simple boundary conditions and one discrete frequency value. For instance, we prescribe a constant pressure amplitude on the Imaginary Boundary, i.e.:

$$p_i = 1000, \tag{3}$$

and a zero pressure at the outlet:

$$p_o = 0. \tag{4}$$

On the rigid walls (which are the spline-shaped encasing outside the rotor and the outer surface along the duct), the particle velocity is set to zero, i.e.:

$$\vec{v}_w = 0. \tag{5}$$

The set of equations (2) - (5) is then solved for the frequency values  $f=440$  Hz and  $f=857.5$  Hz.

Three different algorithms have been used for solving the problem given above, namely: the COMSOL software [4], Boundary Element Method and the Local Boundary Integral Equation (LBIE) method [8].

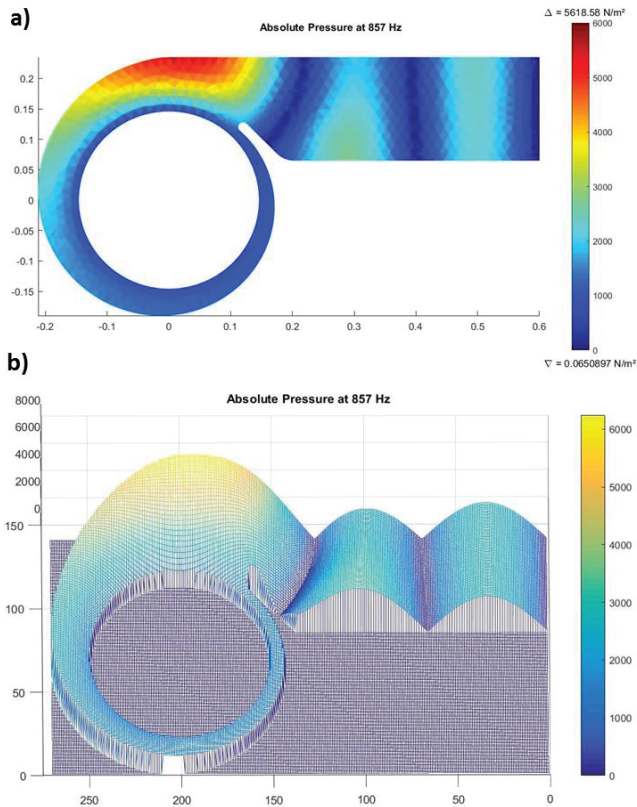


**Figure 5:** The results for the acoustic pressure distribution at 857 Hz for the test problem. (a) The solution with BEM, and (b) the solution with LBIE. Hint: Note that different colour-maps are used in (a) and in (b).

The results are shown in Fig. 4 and 5 for 440 Hz and 857.5 Hz, respectively, along the middle-cut plane in the  $x$ - $y$  direction. Good agreement has been found between the three

methods, observing similar acoustic pressure distribution and amplitude within the domain. The wavelength is approximately comparable to the length of the exhaust duct for the former case (440 Hz). Clearly, higher order modes of propagation are observed as the frequency increases to 857.5 Hz.

**Acoustic calculations using CFD data**

In this section, the hybrid computation of the sound pressure level within the fan is presented. Namely, the results obtained in the time domain for the pressure by the ANSYS CFD simulation on the surfaces of the acoustic computation domain are converted into frequency domain and are used in the boundary element (BEM) code in order to compute the acoustic pressure at the locations inside the fan (see Fig. 6). As mentioned before, the time step for the SST-SAS simulation with  $1^\circ$  rotation is  $5.5 \times 10^{-4}$  s. The last three revolutions of the rotor are taken into account and the data is exported every second time step. Therefore, the cut-off frequency in the frequency domain is 4545 Hz, the total number of time steps is 541, and the frequency resolution is 8.4 Hz.

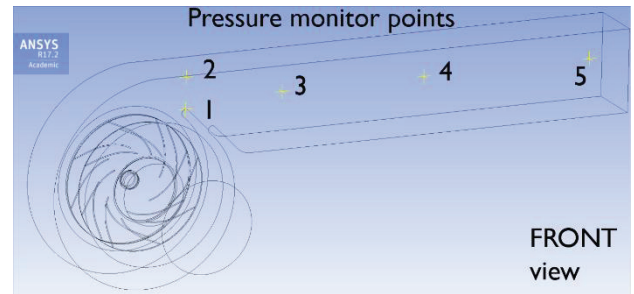


**Figure 6:** The locations of the pressure monitor points

In Fig. 7, the results for the sound pressure level in the domain related to the SST-SAS simulation are shown. The coordinates of the Monitor Point 1 considered in Fig. 7a are  $x=0.110$  m,  $y=0.135$  m and  $z=0.020$  m, whereas Fig. 7b displays the values at the Monitor Point 3 at  $x=0.300$  m,  $y=0.160$  m and  $z=0.050$  m. The red lines in the figure represent the spectrum obtained directly from the time domain CFD data, and the blue lines show the values computed with the BEM at the same points.

At the former location, which is near the volute tongue of the fan, the results seem to agree very well except at frequencies below the Blade Passing Frequency (BPF). The values predicted at the BPF by the CFD simulation and the acoustic simulation are approximately 100 dB and 95 dB, respectively. At the second location, which is towards the middle of the duct of the fan, a good agreement between the CFD and the acoustics results is also found for the whole frequency range. The predicted sound pressure level at the BPF is approximately 98-100 dB with both simulations. The discrepancies observed near the volute tongue at low frequencies (Fig. 7a) may be attributed to the turbulence effects which are more pronounced at this region (Fig. 3a). This latter fact will be investigated in more detail in future

work by taking into account the vortex-related sound sources within the volume.

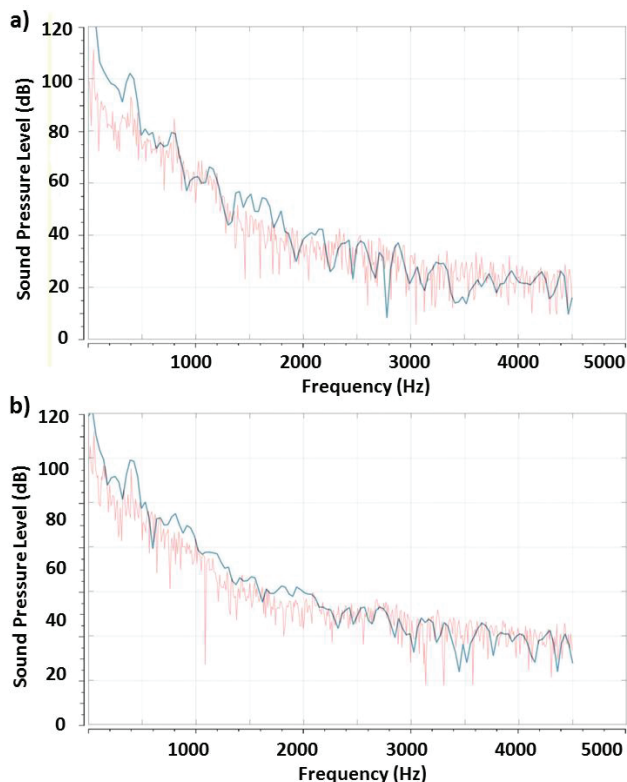


**Figure 7:** The sound pressure level obtained with the CFD simulation (red line) and the acoustic simulation (blue line) at the locations (a)  $x=0.110$  m,  $y=0.135$  m and  $z=0.020$  m, and (b)  $x=0.300$  m,  $y=0.160$  m and  $z=0.050$  m.

## Conclusions and Discussions

In this work, the initial investigations on the computations of the acoustic noise radiated by a laboratory scale radial fan with backward curved blades have been shown. First, the flow through the fan is simulated using the computational fluid dynamics software ANSYS. Then, the results obtained for the pressure variations on the side walls, on the virtual surface outside the rotor, and at the exit of the fan are used for predicting the sound pressure levels at some locations inside the fan. Three different methods have been employed for the CFD simulations: SST-SAS, Detached Eddy Simulation and Stress Blended Eddy Simulation. The turbulent kinetic energy distribution and the velocity field within the fan have been shown. A test case problem is described for the acoustic propagation and solved with COMSOL, Boundary Element Method and the LBIE method. The results obtained using these methods for the acoustic propagation modes at 440 Hz and 857 Hz have shown good agreement. The sound pressure level prediction using the CFD data on the boundaries, though, have been made using the Boundary Element Method.

For the current analysis, the inhomogeneities such as the vortices within the flow have been neglected when computing the acoustic wave propagation. Further stages of this study will aim to take into account the contributions from these sound sources, e.g. as suggested in Ref. [9]. Moreover, several other turbulence models will be

implemented for the fluid flow calculations in order to resolve the details of the air flow. Finally, the ultimate purpose of the current research is to build up the proposed backward curved radial fan, to compare the noise spectrum obtained from experiments with the ones calculated numerically, and to optimize the operating conditions of the fan with respect to its efficiency and the radiated noise.

## Acknowledgements

The authors wish to thank the BMBF and the project partners ANSYS, B/S/H and GRONBACH for their support.



## Literature

- [1] Darvish M.: Numerical and Experimental Investigations of the Noise and Performance Characteristics of a radial Fan with Forward-Curved Blades, Dissertation, TU Berlin, 2015
- [2] Stuchlik A., Frank S.: Numerische Berechnung und Auslegung von Trommelläufer-Ventilatoren (NUBAT), Forschungsbericht, HTW Berlin, 2011, ISBN 978-3-86262-011-1
- [3] Darvish, M.; Frank, S.; Paschereit, C. O.: Numerical and experimental study on the tonal noise generation of a radial fan. *Journal of Turbomachinery* 137(101005) (2015), 1-9
- [4] COMSOL Multiphysics, URL: <https://www.comsol.com/acoustics-module>
- [5] ANSYS – CFX, URL: <http://www.ansys.com/Products/Fluids/ANSYS-CFX>
- [6] Piscocya, R.; Brick, H.; Oehmann, M.; Költzsch, P.: Equivalent source method and boundary element method for calculating combustion noise. *Acta Acustica United with Acustica* 94 (2008), 514-527
- [7] Sorguven, E.; Dogan, Y.; Bayraktar, F.; Sanliturk, K. Y.: Noise prediction via large eddy simulation: Application to radial fans. *Noise Control Engineering Journal* 57(3) (2009), 169-178
- [8] Dogan, H.; Popov, V.; Ooi, E. H.: Dispersion analysis of the meshless local boundary integral equation and radial basis integral equation methods for the Helmholtz equation. *Engineering Analysis with Boundary Elements* 50 (2016), 360-371
- [9] Oberai, A. A.; Roknaldin, F.; Hughes, T. J. R.: Computational procedures for determining structural-acoustic response to hydrodynamic sources. *Computational Methods in Applied Mechanical Engineering* 190 (2000), 345-361